

# Selective Oxidation of Glycerol Catalyzed by Rh/Activated Carbon: Importance of Support Surface Chemistry

Elodie G. Rodrigues · Sónia A. C. Carabineiro ·  
Xiaowei Chen · Juan J. Delgado · José L. Figueiredo ·  
Manuel F. R. Pereira · José J. M. Órfão

Received: 9 October 2010 / Accepted: 22 November 2010 / Published online: 14 December 2010  
© Springer Science+Business Media, LLC 2010

**Abstract** Noble metal catalysts (Pt, Ir, Pd, Rh, Au) supported on activated carbon were assessed for glycerol oxidation. Rhodium is a highly efficient catalyst when the support has neutral or basic properties. The surface chemistry of activated carbon plays a key role in the performance.

**Keywords** Glycerol · Oxidation · Noble metals · Rhodium · Activated carbon · Surface chemistry

## 1 Introduction

The growing concern about global warming leads to numerous discussions about sources of energy. The use of renewable feedstocks is essential for the sustainable development of society, since fossil energy resources are limited. Over the last decade, biodiesel has emerged as a viable clean fuel. It is obtained by transesterification with methanol of triglycerides extracted from seed oils, leaving glycerol as the main by-product. In this process, about 100 kg of glycerol are produced for every ton of biodiesel [1]. During the last years the market for biodiesel was continuously increasing, and it is expected that this trend remains [2]. Consumption of the surplus of glycerol is a necessary requisite for the commercial viability of biodiesel production [3]. The conversion of glycerol into high-value chemicals is a research area that has received tremendous attention in recent years, as a result of glycerol's unique structure, properties, bioavailability and renewability [2, 4, 5]. Liquid phase catalytic oxidation is a promising route to convert glycerol into useful compounds, provided that the catalyst used is sufficiently active and selective for the formation of chemicals such as glyceric acid (GLYCEA) and/or dihydroxyacetone (DIHA), potentially useful as chemical intermediates in the fine chemicals industry, particularly in pharmaceuticals [2, 6]. Until now, these products are being produced by expensive and non-environmentally safe oxidation processes, or by low productivity microbial fermentation processes [7]. However, the extensive functionalization of this molecule, with similar reactive hydroxyl groups, renders its selective oxidation particularly difficult [8].

In recent years, there have been many studies dealing with the oxidation of glycerol to chemical intermediates using supported catalysts with noble metal nanoparticles,

---

E. G. Rodrigues · S. A. C. Carabineiro ·  
J. L. Figueiredo · M. F. R. Pereira · J. J. M. Órfão (✉)  
Laboratório de Catálise e Materiais (LCM), Laboratório  
Associado LSRE/LCM, Departamento de Engenharia Química,  
Faculdade de Engenharia, Universidade do Porto,  
Rua Dr. Roberto Frias, 4200-465 Porto, Portugal  
e-mail: jjmo@fe.up.pt

E. G. Rodrigues  
e-mail: elodie.rodrigues@fe.up.pt

S. A. C. Carabineiro  
e-mail: scarabin@fe.up.pt

J. L. Figueiredo  
e-mail: jlfig@fe.up.pt

M. F. R. Pereira  
e-mail: fpereira@fe.up.pt

X. Chen · J. J. Delgado  
Departamento de Ciência de los Materiales e Ingeniería  
Metalúrgica y Química Inorgánica, Facultad de Ciencias,  
Universidad de Cadiz, Campus Río San Pedro Puerto Real,  
11510 Cadiz, Spain  
e-mail: xiaowei.chen@uca.es

J. J. Delgado  
e-mail: juanjose.delgado@uca.es

such as Pd, Pt and mainly Au on diverse supports [9–15]. The main product of glycerol oxidation using platinum supported on activated carbon is GLYCEA (selectivity 55% at 90% conversion) with a small amount of DIHA (selectivity 12%) [11]. Pd catalysts supported on activated carbon under basic conditions have a high selectivity towards GLYCEA (77 at 90% conversion), whereas the selectivities to the other reaction products (including DIHA) are always lower than 10% [11]. The main disadvantage of catalysts that are based on these metals is their deactivation at increasing reaction time due to oxygen poisoning [12, 16]. On the other hand, gold has a better resistance to oxygen poisoning compared to platinum, allowing for the use of high oxygen partial pressures [17]. However, the catalytic activity of gold depends mainly on nanoparticle sizes, which in turn depend on the preparation method used [12, 18].

Under alkaline conditions, catalyst activity and selectivity seem to be influenced by the nature of the metal, nanoparticle sizes and support. However, catalytic oxidation of glycerol has been investigated by several research groups under different reaction conditions (pH, temperature, oxidants, etc.) with different metals and different supports, leading to a difficult catalyst evaluation and comparison, since many parameters influence catalyst performance. Therefore, this work begins with a comparative study among catalysts under the same reaction conditions and preparation method. Additionally to metals already studied in the literature (platinum, palladium and gold), two other metals (iridium and rhodium) were tested in the glycerol oxidation reaction. Moreover, the influence of the activated carbon surface chemical groups on the rhodium catalyst performance was evaluated. For this purpose, the support surface was modified by appropriate chemical and thermal treatments. The possible role of the surface functional groups of the support in the reaction mechanism was also considered.

## 2 Experimental

### 2.1 Catalysts Preparation

#### 2.1.1 Materials

The metal precursors  $\text{H}_2\text{PtCl}_6$  (99.9% ACS, Pt min 37.5%),  $\text{PdCl}_2$  (99.9% ACS, Pd min 59.5%),  $\text{RhCl}_3$  (99.9% ACS, Rh 38.5–45.5%),  $(\text{NH}_4)_3\text{IrCl}_6$  (99.9% ACS, Ir 38–42%) and  $\text{HAuCl}_4 \cdot 3\text{H}_2\text{O}$  (99.99% ACS, Au min 49.5%) were supplied by Alfa Aesar.

$\text{NaBH}_4$  of purity >95% from Riedel-de Haën,  $\text{NaOH}$  (>97%) and polyvinylalcohol (PVA) (purity > 99%) from Aldrich were also used. The commercial activated carbon

NORIT ROX 0.8 was selected as starting material for the preparation of supports with different surface chemistries.

#### 2.1.2 Preparation Procedures

Gold, iridium, palladium, platinum and rhodium catalysts were prepared by incipient wetness impregnation on the commercial activated carbon. In addition, a gold catalyst was also prepared via the sol immobilization method [19].

The NORIT ROX 0.8 activated carbon has a small amount of surface oxygenated groups. In order to evaluate if the activity of the catalysts correlates with the concentration of oxygenated surface functional groups, the original support was modified by chemical and thermal treatments to obtain supports with different surface chemical properties. Rhodium was supported on these modified activated carbon materials.

**2.1.2.1 Preparation of Supports** A NORIT ROX 0.8 activated carbon (pellets of 0.8 mm diameter and 5 mm length) was used as starting material for this study (sample  $\text{AC}_0$ ). This material was submitted to different chemical and thermal treatments. Both liquid phase oxidations and thermal treatments have been reported not to significantly change the textural properties of activated carbons [20, 21].

An adequate amount of sample  $\text{AC}_0$  was introduced in a Soxhlet extraction apparatus connected to a boiling flask, with a nitric acid 6 M solution, and to a condenser. The reflux was stopped after 3 h. The oxidized material was subsequently washed with distilled water until neutral pH, and then dried at 110 °C for 24 h (sample  $\text{AC}_1$ ). The purpose of this liquid phase oxidation is to increase the amount of oxygen-containing surface groups on the support.

All the thermal treatments were performed on sample  $\text{AC}_1$ , since it is important that the starting material presents a large amount of surface groups in order to produce activated carbons with a high basic character by heat treatment at high temperatures [22]. Support  $\text{AC}_1$  was treated under nitrogen flow for 30 min at different temperatures (400, 600 or 900 °C) followed by treatment under dry air flow at room temperature for 1 h. These thermal treatments selectively remove the oxygen-containing surface groups previously introduced [20, 21]. The final treatment in air is intended to stabilize the surface chemistry of the samples. The following samples were obtained:  $\text{AC}_{1\text{tt}400}$ — $\text{AC}_1$  thermally treated under nitrogen flow at 400 °C for 30 min plus 1 h under dry air flow at room temperature;  $\text{AC}_{1\text{tt}600}$ —similar to  $\text{AC}_{1\text{tt}400}$  but with treatment at 600 °C;  $\text{AC}_{1\text{tt}900}$ —similar to the others but treated at 900 °C. These treatments were carried out in order to remove selectively the oxygen-containing groups on the surface, while maintaining the original textural properties as far as possible.

Before use, all samples were ground to a particle diameter between 0.1 and 0.3 mm in order to minimize mass transfer resistance effects.

**2.1.2.2 Preparation of Catalysts** Au, Pt, Pd, Rh and Ir catalysts were prepared by incipient wetness impregnation of activated carbon with aqueous solutions of the corresponding metallic precursors ( $\text{HAuCl}_4$ ,  $\text{H}_2\text{PtCl}_6$ ,  $\text{PdCl}_2$ ,  $\text{RhCl}_3$ ,  $(\text{NH}_4)_3\text{IrCl}_6$ ). The amount of noble metal was calculated to obtain a nominal metal loading of 1 wt%. In a complementary study, Au catalyst was also prepared by the sol immobilization method with  $\text{NaBH}_4$  as reducing agent (Auc). Briefly,  $\text{HAuCl}_4 \cdot 3\text{H}_2\text{O}$  (35.1 mg) was dissolved in 690 mL of  $\text{H}_2\text{O}$ , and polyvinyl alcohol was added (1.6 mL, 0.2 wt%) under stirring.  $\text{NaBH}_4$  (4 mL, 0.1 M) was added to the yellow solution under vigorous magnetic stirring. The resulting sol was ruby-red in color. Within a few minutes of sol generation, the colloid was immobilized by adding the support under vigorous stirring. The amount of support was calculated to reach a final metal loading of 1 wt%. After 3–4 days, the colorless solution was filtered, the catalyst washed thoroughly with distilled water until the filtrate was free of chloride ( $\text{AgNO}_3$  test) and dried at 110 °C for 24 h [19].

After heat treatment under nitrogen flow for 3 h, the catalysts were activated by reduction under hydrogen flow for 3 h. The appropriate reduction temperature for each catalyst was determined by temperature programmed reduction (TPR), namely 250 °C for the Pd catalyst, 350 °C for Ir, Pt and Au catalysts and 200 °C for Rh catalysts (see Sect. 2.2.2). The treatment under nitrogen flow was carried out at the same temperature used for the reduction.

A supplementary catalyst, called  $\text{Rh/PTAC}_{1\text{tt}600}$ , was also prepared. It was obtained similarly to  $\text{Rh/AC}_1$  as follows: while  $\text{Rh/AC}_1$  was heat-treated under nitrogen at 200 °C,  $\text{Rh/PTAC}_{1\text{tt}600}$  was heat-treated at 600 °C before reduction at 200 °C.

An additional catalyst (Au/C), provided by the World Gold Council, was used as reference. Data sheets accompanying this sample indicate that it was prepared by the sol method and has a metal load of 0.8 wt%; the support is a carbon black. This catalyst was used without any additional treatment.

## 2.2 Characterization of Supports and Catalysts

The supports were characterized by  $\text{N}_2$  adsorption at  $-196$  °C, temperature programmed desorption (TPD) and by determination of the pH at the point of zero charge ( $\text{pH}_{\text{pzc}}$ ). The catalysts were also characterized by temperature programmed reduction (TPR). Samples that showed the most interesting catalytic performances were further

characterized by microscopy and inductively coupled plasma (ICP) analysis.

### 2.2.1 $\text{N}_2$ Adsorption

Textural characterization of the samples was based on the analysis of nitrogen adsorption isotherms, measured at  $-196$  °C in a NOVA 4200e Quantachrome Instruments apparatus. BET surface areas ( $S_{\text{BET}}$ ) were calculated, as well as micropore volumes ( $V_{\text{micro}}$ ) and mesopore surface areas ( $S_{\text{meso}}$ ) according to the *t*-method.

### 2.2.2 Temperature Programmed Reduction (TPR)

Temperature programmed reduction allows to find the most adequate reduction temperature for each metal. TPR profiles were obtained with a fully automated AMI-200 (Altamira Instruments). The catalyst (150 mg) was placed in a U-shaped quartz tube inside an electrical furnace and submitted to a  $5$  °C  $\text{min}^{-1}$  linear temperature increase up to 600 °C under 5% (v/v) hydrogen flow diluted in helium (total flow rate =  $30$   $\text{Ncm}^3$   $\text{min}^{-1}$ ). A thermal conductivity detector and a quadrupole mass spectrometer (Dymaxion 200, Ametek) were used to monitor the change in composition of the reactor effluent.  $\text{H}_2$  consumption peaks indicate directly the temperature ranges where reduction occurs. The selected reduction temperatures are indicated in Sect. 2.1.2.2.

### 2.2.3 Surface Chemistry Characterization

The qualitative and quantitative determination of oxygenated surface functional groups was performed by temperature programmed desorption—mass spectrometry (TPD-MS) [20, 21]. CO and  $\text{CO}_2$  TPD spectra were obtained with the fully automated AMI-200 (Altamira Instruments) already mentioned. The samples (150 mg) were placed in a U-shaped quartz tube inside an electrical furnace and subjected to a  $5$  °C  $\text{min}^{-1}$  linear temperature increase up to 1100 °C under helium flow ( $25$   $\text{Ncm}^3$   $\text{min}^{-1}$ ). A quadrupole mass spectrometer (Dymaxion 200, Ametek) was used to monitor CO and  $\text{CO}_2$  signals. For quantification of the CO and  $\text{CO}_2$  released, calibration of these gases was carried out at the end of each analysis.

The determination of the pH at the point of zero charge ( $\text{pH}_{\text{pzc}}$ ) of the samples was carried out as follows [23]. 50 mL of NaCl 0.01 M solution was introduced in closed Erlenmeyer flasks. The pH was adjusted to a value between 2 and 12 by adding HCl 0.1 M or NaOH 0.1 M solutions. Then, 0.15 g of the carbon sample was added and the final pH measured after 48 h under agitation at room temperature. Blank experiments (without addition of support) were also prepared for each pH, and the values measured after 48 h correspond to  $\text{pH}_{\text{initial}}$ . The  $\text{pH}_{\text{pzc}}$  is the point where the

curve  $\text{pH}_{\text{final}}$  versus  $\text{pH}_{\text{initial}}$  crosses the line  $\text{pH}_{\text{final}} = \text{pH}_{\text{initial}}$ .

### 2.2.4 Microscopy

Transmission electron microscopy (TEM) measurements were performed for the most promising catalysts in a JEOL2010F instrument, with 0.19 nm spatial resolution at Scherzer defocus conditions. High Angel Annular Dark Field—Scanning Transmission Electron Microscopy (HAADF-STEM) images were obtained with the same microscope. An electron probe with diameter of 0.5 nm at a diffraction camera length of 10 cm was used for the HAADF mode. The samples were deposited on the Cu grids coated holey-carbon for TEM analysis.

### 2.2.5 Inductively Coupled Plasma (ICP)

The metal loadings of the prepared catalysts were determined in duplicate by ICP, using an Iris Intrepid Spectrometer (Thermo Elemental). An Ethos 1600 microwave labstation (Milestone) was used to prepare the acid solution of all the samples for ICP analysis.

### 2.3 Catalysts Evaluation

The reaction tests were performed in a 350 mL stainless steel reactor equipped with manometer, temperature sensor, magnetic stirrer and sample outlet. The oxidation reactions were carried out with oxygen under pressure up to 10 bar and at temperatures from 40 to 100 °C. NaOH solution (NaOH/glycerol molar ratio = 2) and catalyst (700 mg) were added to a 0.3 M aqueous solution of glycerol ( $V = 150$  mL) under stirring at 1000 rpm. Preliminary experiments show that external mass transfer limitations were overcome at this stirring speed. After heating under nitrogen to the desired temperature, the reaction was initiated by switching from inert gas to oxygen. The reaction was monitored by taking samples (0.5 mL) for analysis at regular time intervals.

The quantitative analysis of the reaction mixtures was carried out by high performance liquid chromatography (HPLC). The chromatograph (Elite LaChrom HITACHI) was equipped with a refractive index and an ultraviolet (210 nm) detector. Reactant and products were separated in an ion exclusion column (Alltech OA 1000). The eluent was a solution of  $\text{H}_2\text{SO}_4$  (0.01 M). An injection volume of 20  $\mu\text{L}$ , a measuring time of 15 min and a flow rate of 0.5  $\text{mL min}^{-1}$  were selected. Products were identified by comparison with standard samples. Glycerol (>99.5%) was purchased from Fluka and all reaction products from Sigma-Aldrich. The selectivities ( $S_i$ ) (also named relative

yields by other authors) into the different products  $i$  at time  $t$  were calculated as:

$$S_i = \frac{C_i / (v \cdot C_0)}{X} \quad (1)$$

where  $C_i$  is the concentration of product  $i$  ( $\text{mol L}^{-1}$ ),  $C_0$  is the initial concentration of glycerol ( $\text{mol L}^{-1}$ ),  $X$  is the glycerol conversion and  $v$  corresponds to the moles of  $i$  produced per mol of glycerol consumed, according to the stoichiometry.

## 3 Results and Discussion

### 3.1 Characterization of Supports and Catalysts

#### 3.1.1 Textural Properties

The textural characterization of the different supports and of the Pd/AC<sub>0</sub> catalyst is presented in Table 1. As expected, no major differences in the textural properties of the materials were observed. The slight decrease in AC<sub>1</sub> surface area may be due to the abundant presence of oxygen-containing groups introduced on the surface of the activated carbon by treatment with  $\text{HNO}_3$ , which possibly block the entry of  $\text{N}_2$  inside the small pores. After treatment at 900 °C (sample AC<sub>1tt900</sub>), the mentioned functional groups were removed by thermal decomposition and the area of the corresponding support increased slightly comparatively to the original carbon [24, 25].

The textural parameters of the Pd/AC<sub>0</sub> catalyst decreased only slightly compared to the unloaded carbon. Therefore, it was assumed that the textural properties of the modified supports and of the supported metal catalysts are not significantly different from those of the original activated carbon.

#### 3.1.2 Surface Chemistry Characterization

The total amounts of the various surface groups (acidic carboxylic acids, carboxylic anhydrides, lactones, phenols,

**Table 1** Textural properties and  $\text{pH}_{\text{pzc}}$  of original and modified activated carbons

Sample	$S_{\text{BET}}$ ( $\text{m}^2 \text{g}^{-1}$ )	$S_{\text{meso}}$ ( $\text{m}^2 \text{g}^{-1}$ )	$V_{\text{micro}}$ ( $\text{cm}^3 \text{g}^{-1}$ )	$\text{pH}_{\text{pzc}}$
AC <sub>0</sub>	1025	180	0.361	7.9
AC <sub>1</sub>	965	156	0.369	3.2
AC <sub>1tt400</sub>	952	200	0.350	n.d.
AC <sub>1tt600</sub>	1042	150	0.391	n.d.
AC <sub>1tt900</sub>	1106	184	0.399	8.2
Pd/AC <sub>0</sub>	887	140	0.366	n.d.

and carbonyls or quinones) on carbon materials can be determined from TPD spectra, since these groups are decomposed upon heating by releasing CO and/or CO<sub>2</sub> in different temperature ranges. Accordingly, it is possible to identify the oxygenated groups on the surface of a given material by TPD experiments. It was reported that CO<sub>2</sub> results from the decomposition of carboxylic acids at low temperatures (150–450 °C) and from lactones at high temperatures (600–800 °C); carboxylic anhydrides originate both CO and CO<sub>2</sub> (400–650 °C); groups such as phenols (600–800 °C), carbonyls and quinones (750–1000 °C) originate CO [20, 21].

Figure 1a and b shows, respectively, the CO and CO<sub>2</sub> TPD spectra of the commercial activated carbon as received (AC<sub>0</sub>) and the modified samples. An increase in the amount of surface oxygenated groups is evidenced by the increase of CO and CO<sub>2</sub> released. Analyzing the results, it is clear that the liquid phase oxidation with HNO<sub>3</sub> significantly increased the amount of CO<sub>2</sub> evolved at low temperatures (carboxylic acid groups) and introduced a large amount of surface oxygen, which decomposes at high temperatures by releasing CO (phenol and carbonyl/quinone groups), originating a support with acidic and hydrophilic characteristics (sample AC<sub>1</sub>) [26]. As

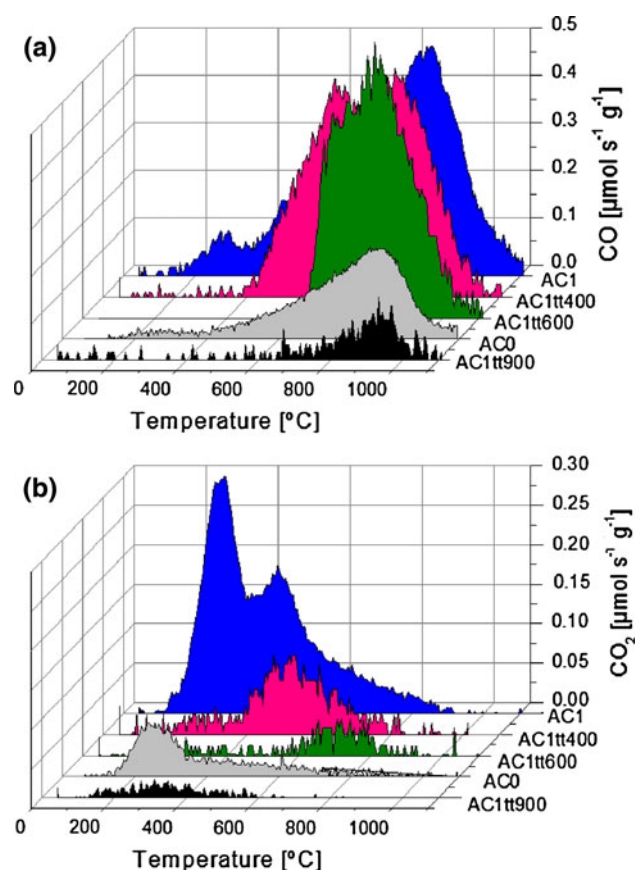


**Fig. 1** TPD spectra of the different activated carbons: **a** CO. **b** CO<sub>2</sub>

expected, the oxidized sample AC<sub>1</sub> has a low pH<sub>pzc</sub> (see Table 1), due to the introduction of the mentioned oxygen-containing functional groups with acidic properties, namely carboxylic acids. Thermal treatments selectively remove those surface groups, originating materials with progressively lower oxygen content. Practically all groups were removed from sample AC<sub>1tt900</sub>, which has basic properties [27]. According to Leon y Leon et al. [28], this basic character is mainly due to the electron rich oxygen-free sites located on the carbon basal planes.

### 3.1.3 Microscopy and ICP Analyses

TEM micrographs were collected in order to get information about the metal particle size distributions (Fig. 2). The average crystallite sizes of the studied catalysts are presented in Table 2. It should be noticed that the value corresponding to Ir/AC<sub>0</sub> was obtained by hydrogen chemisorption; details of the experimental technique used can be found elsewhere [29]. When using the incipient wetness method it was possible to obtain relatively small metal crystallite sizes for the catalysts prepared. The only exception was the gold catalyst, which required a different method for promoting a high dispersion. It is well-known [12] that sizes of gold nanoparticles mainly depend on the synthesis method used. For instance, the conventional impregnation technique (incipient wetness) results in much larger gold particles than the sol immobilization method (50 nm vs. 6.8 nm). This is in part due to the negative effect of the chloride involved in the preparation, which results in poisoning and excessive sintering of the Au particles [30]. This does not occur in the case of the other noble metals, for which the incipient wetness method allows to produce well-dispersed nanoparticles.

A large amount of oxygen-containing groups on the activated carbon surface can influence the metal dispersion. The surface oxygen groups were considered to act as anchoring sites that interact with metallic precursors [31]. However, the functional groups present on activated carbon are easily decomposed upon heating even at low temperatures. This occurs with some carboxylic acid groups, which already decompose at temperatures below 200 °C, as it can be seen in the TPD spectra (Fig. 1, sample AC<sub>1</sub>). When the catalysts are submitted to heat treatment and reduction processes, these oxygenated groups are thermally decomposed and the rhodium particles that were anchored to them may have low stability and could be prone to sintering. This can possibly explain why Rh/AC<sub>1</sub> and Rh/PTAC<sub>1tt600</sub> catalysts have larger metallic particles than Rh/AC<sub>0</sub>, Rh/AC<sub>1tt600</sub> and Rh/AC<sub>1tt900</sub>, because on this latter group of samples, contrarily to the former, there was no oxygenated groups that decompose at low temperatures during the preparation step.

**Fig. 2** Particle sizes distribution of **a** Pd/AC<sub>0</sub>, **b** Pt/AC<sub>0</sub>, **c** Au/AC<sub>0</sub>, **d** Rh/AC<sub>0</sub>, **e** Rh/AC<sub>1</sub>, **f** Rh/AC<sub>1tt600</sub>, **g** Rh/PTAC<sub>1tt600</sub> and **h** Rh/AC<sub>1tt900</sub>. In some cases the HAADF-STEM images are inserted

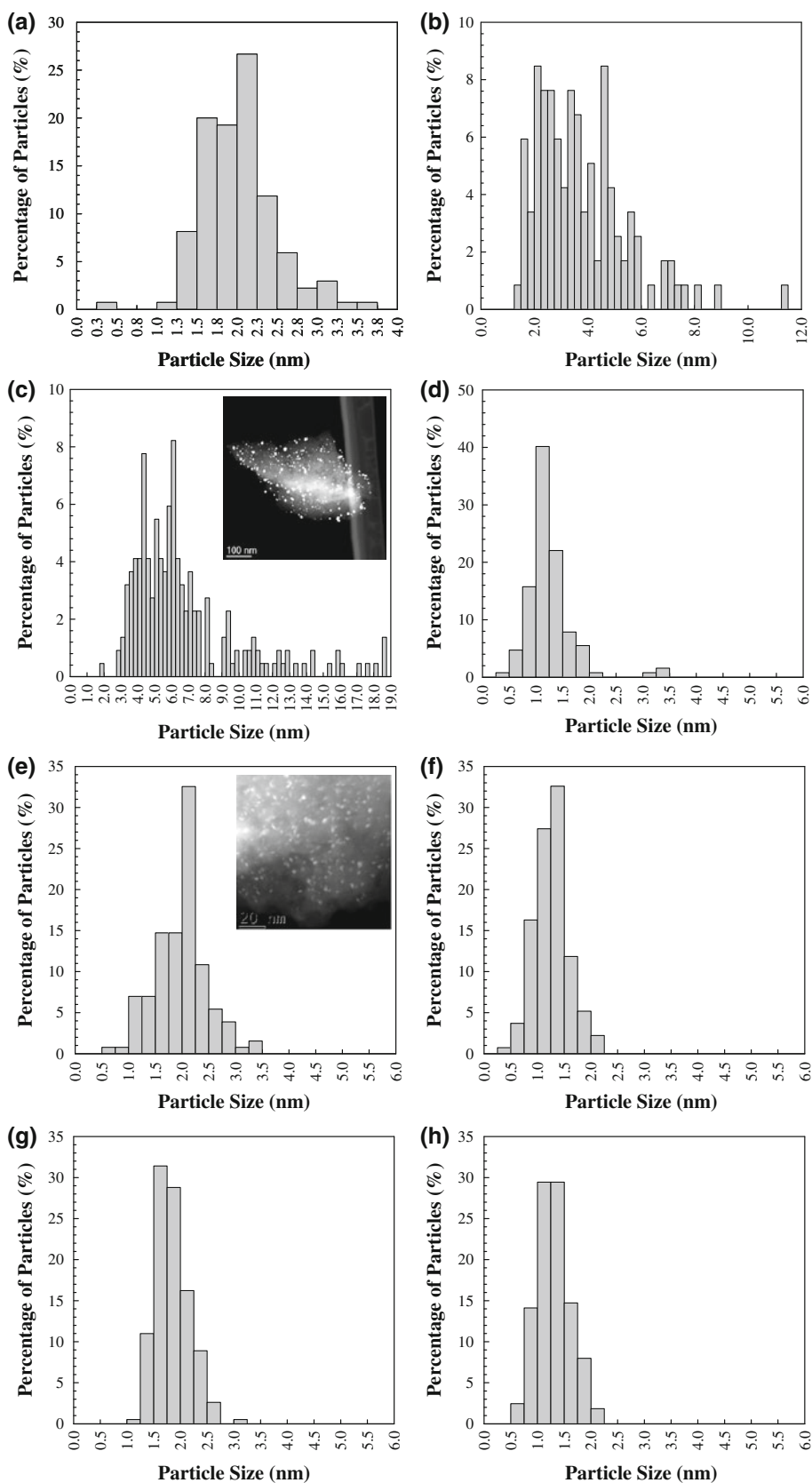


**Table 2** Average crystallite size and metal content of the studied catalysts

Catalyst	Metal loading (%)	$d_M$ (nm)
Pd/AC <sub>0</sub>	0.65 ± 0.03	2.0
Pt/AC <sub>0</sub>	0.50 ± 0.02	3.8
Ir/AC <sub>0</sub>	n.d.	1.7 <sup>a</sup>
Au/AC <sub>0</sub>	n.d.	50
Auc/AC <sub>0</sub>	0.32 ± 0.05	6.8
Rh/AC <sub>0</sub>	0.74 ± 0.05	1.3
Rh/AC <sub>1</sub>	0.74 ± 0.01	2.0
Rh/AC <sub>1tt600</sub>	0.74 ± 0.01	1.3
Rh/AC <sub>1tt900</sub>	0.78 ± 0.01	1.3
Rh/PTAC <sub>1tt600</sub>	0.70 ± 0.03	1.8
Au/C	0.8	11

<sup>a</sup> Obtained by hydrogen chemisorption

Table 2 summarizes the metal loading of some of the catalysts. Regarding to the sol immobilization method, the electrostatic interaction between the stabilized Au particles and the support play an important role during the preparation [32]. The pH of the gold sols was about six. At this pH the zeta potential of gold sols is negative [32] while the surface charge of activated carbon is only slightly positive, considering that their  $pH_{pzc}$  is 7.9. Thus, the interaction between the support and the gold sol was relatively weak, which can explain the low loading of the Auc/AC<sub>0</sub> catalyst.

Chemical and heat-treatments of activated carbon did not influence substantially the metal content of rhodium catalysts.

## 3.2 Oxidation Experiments

### 3.2.1 Catalyst Evaluation

Many parameters play a role in determining the activity of catalysts in the liquid phase oxidation of glycerol. It is not easy to compare the performances of catalysts that are tested under widely different conditions, as reported in the literature. Therefore, in the first part of this work, several metals were supported on activated carbon AC<sub>0</sub>, using the same preparation method (incipient wetness), and the same operational conditions were maintained in all catalytic tests.

The conversion of glycerol on AC<sub>0</sub> supported catalysts was studied as a function of time for different metals. Using typical conditions (60 °C, 3 bar, 150 mL of glycerol 0.3 M, NaOH/glycerol = 2 mol/mol, catalyst amount = 700 mg), the performances presented in Fig. 3 were obtained, which decrease in the order: Pd > Rh >> Pt. Under the conditions tested, Ir and Au prepared by incipient wetness are not active. Even though platinum has a dispersion slightly

lower than palladium and rhodium, the low performance observed is probably due to oxygen poisoning, which is directly related to the oxygen partial pressure, as mentioned in the literature [11]. This can also explain the inactivity of the iridium catalyst. However, according to van Dam et al. [33], metals with a higher oxidation potential are less prone to oxidation. Thus, among the metals tested, platinum would be the less easily poisoned by over-oxidation, followed by iridium, palladium and rhodium, which was not verified. Actually, incipient wetness allows obtaining very active Pd and Rh catalysts in a simple, easy and quick way; these catalysts promote a high glycerol conversion even at a working pressure of 3 bar. The absence of deactivation by oxygen on various platinum-group metals due to strong metal-substrate interactions has already been reported [34]. So, the high activity obtained can possibly be attributed to the high affinity of glycerol for rhodium and palladium, which limits oxygen adsorption. This is particularly interesting, since no study concerning rhodium catalysts for glycerol oxidation has been published previously.

Contrarily to the other catalysts prepared by the incipient wetness method, the gold catalyst was the only that presented low particle dispersion. This can explain its inactivity once, as already mentioned, well-dispersed gold nanoparticles are required in order to obtain an active catalyst. Therefore, to study the influence of the preparation method on the gold catalyst performance, a sol immobilization method was applied. From TEM analysis (Table 2), it was concluded that this method appears to be suitable for generating small crystallite sizes supported on active carbon, originating an active catalyst as it can be observed in Fig. 3. When comparing with the reference Au/C catalyst, Auc/AC<sub>0</sub> exhibits a much higher activity. In

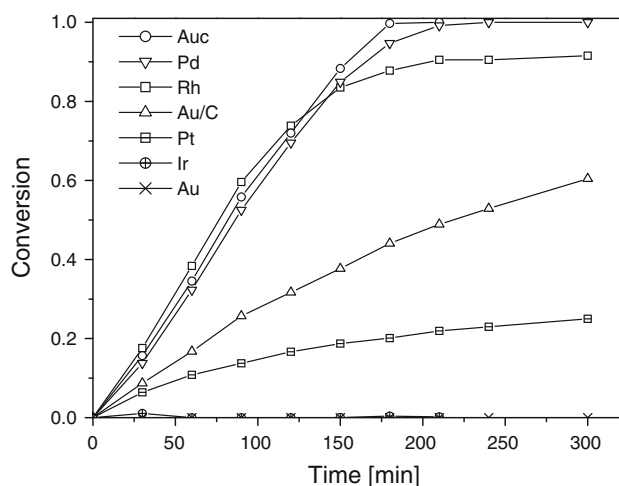


**Fig. 3** Oxidation of glycerol over noble metal catalysts supported on activated carbon AC<sub>0</sub>. Reaction conditions: 60 °C,  $p_{O_2}$  = 3 bar, 150 mL of glycerol 0.3 M, NaOH/glycerol = 2 mol/mol, catalyst amount = 700 mg

fact, after 3 h, this gold catalyst supported on activated carbon is able to reach 100% glycerol conversion, whereas only 44% is achieved with Au/C. This can be explained by the larger gold particles of the latter catalyst (11 nm vs. 6.8 nm), but a support effect can also influence its performance, since these gold particles are supported on carbon black. It should be noted that the prepared Auc/AC<sub>0</sub> has a remarkable catalytic activity, particularly considering its low metal loading (0.32%).

The selectivities to products obtained in the presence of the different catalysts are compared in Table 3 at constant reaction time (3 h), since the selectivities to the main products changed only slightly during the reaction. However, for comparison purposes, Table 3 also shows the selectivities at the same glycerol conversion (25%). The evolution of DIHA and GLYCEA selectivities as a function of time in the presence of Rh/AC<sub>0</sub> can be seen in Fig. 4. The prepared catalysts lead to a high total selectivity of about 75–80% to products of commercial interest (GLYCEA + DIHA), and a very similar distribution of the products was observed independently of the nature of the metal. Besides the desired GLYCEA and DIHA, glycolic acid (GLYCOA), glyceraldehyde (GLYCER) and tartronic acid (TARTA) were also measured; oxalic acid was detected in some cases, but always with very low concentrations. The selectivity to GLYCEA is higher than to DIHA for all the catalysts prepared (around 60% after 3 h). The selectivities to GLYCOA and to DIHA are similar (between 10 and 20%). The performance of the reference Au/C catalyst differs, as it seems to promote almost in the same way the oxidation of primary and secondary alcohol functions, since the observed selectivities to DIHA and GLYCEA after 3 h are 38 and 42%, respectively.

### 3.2.2 Influence of Pressure and Temperature

A more detailed study was carried out with the rhodium catalyst, which as far as we are aware is reported here for the first time as active in glycerol oxidation. The influence of oxygen pressure and temperature on the reaction kinetics

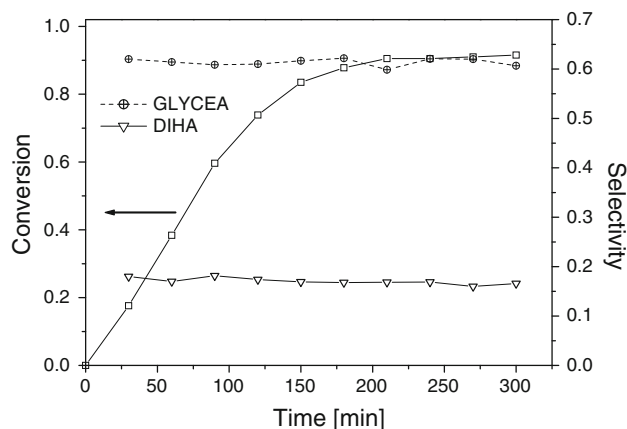


**Fig. 4** Evolution of DIHA and GLYCEA selectivities and glycerol conversion during the reaction in the presence of the Rh/AC<sub>0</sub> catalyst

was examined. The aim of this investigation was to establish the dependency of the reaction rate and catalyst selectivity on the oxygen pressure and reaction temperature for the Rh/AC<sub>0</sub> catalyst.

Experiments were carried out with 150 mL of glycerol (0.3 M), NaOH/glycerol ratio = 2 mol/mol and 700 mg of catalysts. The oxygen pressure was varied between 3 and 10 bar and the temperature between 40 and 100 °C.

Under the tested conditions, it was found that the oxygen pressure influences significantly the reaction rates of glycerol oxidation (Fig. 5a). The initial reaction rate increases with the oxygen pressure but the catalyst deactivates more readily. Increasing the oxygen pressure seems to lead to a higher oxygen coverage of the surface, and thus to a premature deactivation of the rhodium catalyst due to oxygen poisoning of the surface. This metal appears to be very sensitive to the amount of oxygen dissolved in the reaction medium. This situation is similar to that described by Garcia et al. [11] for Pt catalysts.

Selectivity to DIHA is slightly increased with the increase of oxygen pressure while selectivity to GLYCOA decreases (Table 4).

The temperature increase leads to an increase of catalytic activity in the system studied (Fig. 5b), but seems to

**Table 3** Product selectivities at  $t = 3$  h and  $X = 25\%$  for glycerol oxidation over noble metal catalysts supported on activated carbon AC<sub>0</sub> and over the Au/C reference catalyst

	t = 180 min					X <sub>GLY</sub> = 25%			
	X <sub>GLY</sub>	S <sub>GLYCEA</sub>	S <sub>GLYCOA</sub>	S <sub>DIHA</sub>	S <sub>TARTA</sub>	S <sub>GLYCEA</sub>	S <sub>GLYCOA</sub>	S <sub>DIHA</sub>	S <sub>TARTA</sub>
Pd	0.95	0.64	0.11	0.16	0.09	0.62	0.12	0.17	0.09
Rh	0.88	0.62	0.15	0.17	0.06	0.61	0.16	0.17	0.06
Pt	0.20	0.60	0.15	0.20	0.04	0.61	0.15	0.21	0.03
Auc	1.0	0.60	0.14	0.18	0.05	0.61	0.16	0.17	0.05
Au/C	0.44	0.42	0.20	0.38	0	0.42	0.21	0.37	0

Reaction conditions: 60 °C,  $p_{O_2} = 3$  bar, 150 mL of glycerol 0.3 M, NaOH/glycerol = 2 mol/mol, catalyst amount = 700 mg

be very detrimental to the selectivity of the most interesting products, especially glyceric acid, which oxidizes very easily to glycolic acid and further to oxalic acid at high temperatures (Table 4). Once again, the results obtained at 40 and 50 °C show that rhodium suffers deactivation resulting from the high level of oxygen present in the reaction medium at these temperatures. It is a common assumption that the mechanism of glycerol oxidation involves an oxidative dehydrogenation step. The last step is the elimination of hydrogen by reaction with dissociatively adsorbed oxygen [35]. Therefore, an increase of the oxygen coverage on the metal surface progressively eliminates glycerol adsorption. Over-oxidation leads to a loss of activity due to the transformation of metal M to  $M^{n+}$ , the conversion reaching a plateau (Fig. 5a, b). However, this deactivation can be eliminated by decreasing the rate of oxygen supply (e.g. by working at higher temperatures [16], as can be seen in Fig. 5b).

In some cases, the sum of the calculated selectivities in Table 4 is lower than one, since some oxalic acid was also detected. It is important to notice that in the experiment with the Rh/AC<sub>0</sub> catalyst at 100 °C, even after accounting

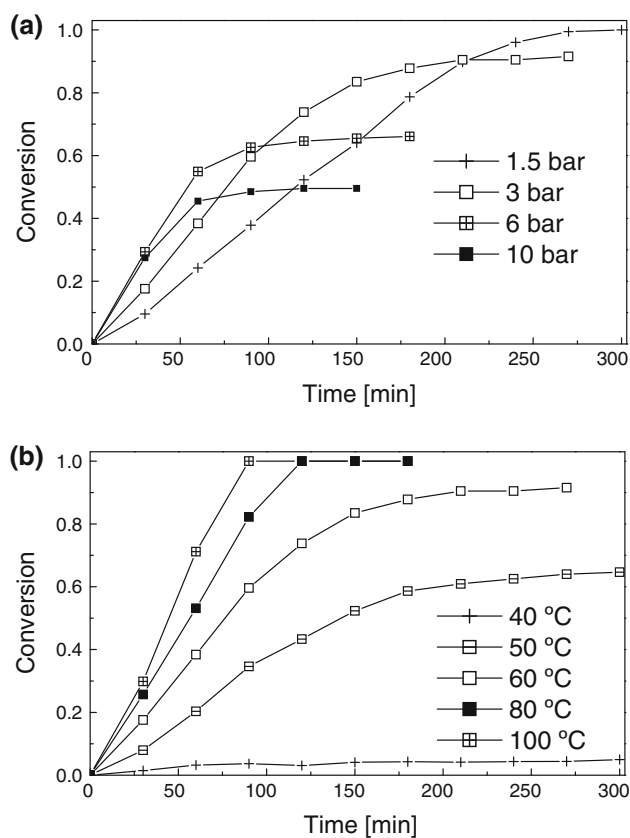


**Fig. 5** Dependency of glycerol conversion on the oxygen pressure at 60 °C (a) and on reaction temperature at  $p_{O_2} = 3$  bar (b) with Rh/AC<sub>0</sub>. Other reaction conditions: 150 mL of glycerol 0.3 M, NaOH/glycerol = 2 mol/mol, catalyst amount = 700 mg

for the oxalic acid formed (selectivity = 0.05), the sum of selectivities is still lower than one. As no additional product was detected by HPLC, we supposed that, in this particular case, some complete oxidation of the partial oxidation products to CO<sub>2</sub> occurs. The formation of CO<sub>2</sub> as a by-product in the glycerol oxidation was also observed by Carretin et al. [9].

It can be concluded that, for rhodium catalyst, a compromise between activity and selectivity has to be achieved using suitable temperature and oxygen pressure in order to avoid problems of over-oxidation.

### 3.2.3 Investigation of the Support Effects in the Glycerol Oxidation

The surface oxygenated functional groups of activated carbon can be controlled by chemical and heat treatments, and can change the catalytic properties. Figure 6 reveals a strong influence of the surface chemical properties of the support on the catalytic performance in glycerol oxidation. It was observed by ICP analysis that the metal loading did not change significantly from support to support. As the textural properties of the support also do not differ substantially, the metal particle sizes were analyzed by TEM to establish differences in metal dispersion (Fig. 2; Table 2). Rh/AC<sub>0</sub>, Rh/AC<sub>1tt600</sub> and Rh/AC<sub>1tt900</sub> catalysts have similar crystallite sizes, which are on average smaller than those of Rh/AC<sub>1</sub> and Rh/PTAC<sub>1tt600</sub>. The differences of metal dispersions in these activated carbon supported rhodium catalysts are mainly related to the oxygen-containing groups anchored on the surface of the support, as already mentioned (see Sect. 3.1.3). However, even though Rh/AC<sub>0</sub>, Rh/AC<sub>1tt600</sub> and Rh/AC<sub>1tt900</sub> catalysts have similar particles sizes, rhodium particles supported on AC<sub>0</sub> exhibit a much higher activity. The histograms of the rhodium particle size distribution for AC<sub>0</sub>, AC<sub>1tt600</sub> and AC<sub>1tt900</sub> supported catalysts are shown in Fig. 2d, f, h, respectively. It can be seen that the distribution of rhodium particle diameters in the Rh/AC<sub>0</sub> catalyst is less homogeneous than those of Rh/AC<sub>1tt600</sub> or Rh/AC<sub>1tt900</sub>. Although most particles have about 1.0–1.5 nm, there are a few particles larger than 2.25 nm that are not present in the other two catalysts. Then, it seems that the deactivation of the Rh/AC<sub>1tt600</sub> and Rh/AC<sub>1tt900</sub> catalysts can be explained by over-oxidation, since small metal nanoparticles (<2 nm) deactivate more readily because of their stronger affinity to oxygen [35]. In fact, in Sect. 3.2.2., it was already observed that rhodium is very sensitive to oxygen. Moreover, an experiment carried out with Rh/AC<sub>1tt900</sub> shows that over-oxidation can be delayed when working at an oxygen pressure of 0.5 bar (see Fig. 6), which confirms that the deactivation observed is

**Table 4** GLYCEA, GLYCOA, DIHA and TARTA selectivities ( $S_{\text{GLYCEA}}$ ,  $S_{\text{GLYCOA}}$ ,  $S_{\text{DIHA}}$ ,  $S_{\text{TARTA}}$ ) at different oxygen pressures and temperatures, for 50% glycerol conversions ( $X_{\text{GLY}}$ ) and after 2 h of reaction in the presence of the Rh/AC<sub>0</sub> catalyst

	t = 120 min					$X_{\text{GLY}} = 50\%$			
	$X_{\text{GLY}}$	$S_{\text{GLYCEA}}$	$S_{\text{GLYCOA}}$	$S_{\text{DIHA}}$	$S_{\text{TARTA}}$	$S_{\text{GLYCEA}}$	$S_{\text{GLYCOA}}$	$S_{\text{DIHA}}$	$S_{\text{TARTA}}$
Rh/AC <sub>0</sub>									
1.5 bar <sup>a</sup>	0.52	0.58	0.21	0.16	0.05	0.58	0.21	0.16	0.05
3 bar <sup>a</sup>	0.74	0.61	0.16	0.17	0.06	0.61	0.16	0.17	0.06
6 bar <sup>a</sup>	0.65	0.61	0.12	0.20	0.07	0.61	0.12	0.20	0.07
10 bar <sup>a</sup>	0.50	0.58	0.13	0.22	0.07	0.58	0.13	0.22	0.07
50 °C <sup>b</sup>	0.43	0.57	0.14	0.23	0.06	0.58	0.14	0.23	0.05
60 °C <sup>b</sup>	0.74	0.61	0.16	0.17	0.06	0.61	0.16	0.17	0.06
80 °C <sup>b</sup>	1.0	0.41	0.20	0.27	0.07	0.43	0.22	0.29	0.06
100 °C <sup>b</sup>	1.0	0.30	0.25	0.28	0.06	0.30	0.25	0.30	0.04

<sup>a</sup> Reaction conditions: 60 °C, 150 mL of glycerol 0.3 M, NaOH/glycerol = 2 mol/mol, catalyst amount = 700 mg

<sup>b</sup> Reaction conditions:  $p_{\text{O}_2} = 3$  bar, 150 mL of glycerol 0.3 M, NaOH/glycerol = 2 mol/mol, catalyst amount = 700 mg

due to oxygen poisoning; however, as expected, the initial reaction rate is much lower. In conclusion, the obtained results suggest that rhodium supported on activated carbon seems to be a suitable catalyst for glycerol oxidation provided that its particles are large enough to avoid over-oxidation. Nevertheless, when considering the Rh/AC<sub>1</sub> catalyst, which has a significant fraction of particles larger than 2 nm, only a residual activity is observed. This indicates that surface acid groups are prejudicial for rhodium catalyst activity. Indeed, when a similar catalyst is prepared and post-heat-treated at 600 °C (instead of 200 °C) before reduction, the more acidic groups are eliminated, and activity increases dramatically, although the average particle size remains approximately the same. This catalyst (Rh/PTAC<sub>11600</sub>) does not have carboxylic acid or carboxylic anhydride groups. Additionally, a Rh/PTAC<sub>11400</sub> catalyst (heat-treated at 400 °C) was prepared in order to remove only carboxylic acids from the surface, but no enhancement of the activity was observed when compared with Rh/AC<sub>1</sub> (data not shown). So, not only carboxylic acid groups (released by thermal treatment up to 400 °C) but also the carboxylic anhydrides (released between 400 and 600 °C) appear to lead to almost inactive catalysts.

Two different deactivation procedures were distinguished: over-oxidation (oxygen poisoning) and the presence of a large amount of surface oxygenated acidic groups. Therefore, rhodium catalysts appear to be suitable for glycerol oxidation, provided that their crystallites are not too small and the support has neutral or basic properties. These two parameters can easily be controlled by thermal treatments.

In terms of selectivity, the presence of oxygenated surface groups on Rh/PTAC<sub>11600</sub> leads to an increase in the selectivity to DIHA when compared with the Rh/AC<sub>0</sub>

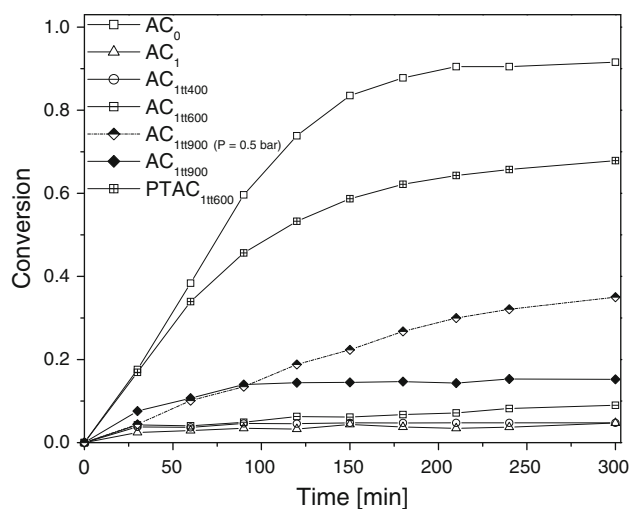


**Fig. 6** Influence of modified activated carbon supports on the activity of rhodium catalysts. Reaction conditions: 60 °C,  $p_{\text{O}_2} = 3$  bar, 150 mL of glycerol 0.3 M, NaOH/glycerol = 2 mol/mol, catalyst amount = 700 mg

catalyst (0.31 vs. 0.17 at  $t = 3$  h and 0.28 vs. 0.18 at  $X = 50\%$ ) and a decrease in the selectivity to GLYCEA (0.53 vs. 0.62 at  $t = 3$  h and 0.56 vs. 0.61 at  $X = 50\%$ ).

The presence of surface groups may cause differences in adsorption performance [36], i.e. the functional groups located near the metal particles can influence glycerol adsorption. The AC<sub>1</sub> support has the largest amount of surface groups, so the Rh/AC<sub>1</sub> catalyst has the most hydrophilic character, and consequently the highest affinity for the aqueous phase. This functionalized carbon surface facilitates adsorption of glycerol from water. So, glycerol may adsorb preferentially on the support and/or functional groups can impede the access of the glycerol molecule to the metal. However, the Rh/PTAC<sub>11600</sub> catalyst shows an increase of activity, in spite of the relatively high content of

oxygenated groups on the surface (despite its less acidic nature). Moreover, a study carried out on AC<sub>0</sub>, without any additional treatment, allowed to conclude that glycerol also adsorbs on this support, and its adsorption is well-represented by the Langmuir isotherm [37]. Then, the adsorption of glycerol on the support does not seem to explain, at least completely, the largely different activities.

Basic carbons are characterized by a high content of electron rich sites on their basal planes and a low concentration of electron withdrawing groups; the presence of oxygen-containing functional groups with electron-withdrawing properties has a negative effect on the adsorption of anionic species [28]. So, assuming that the glycerol oxidation mechanism on rhodium involves the spillover of activated oxygen from the metal to the support, Rh/AC<sub>1</sub> is the catalyst with the lower capacity to accept these species. Therefore, Rh/AC<sub>1</sub> cannot store oxygen, as the support is already oxygenated, and the reaction will stop; on the contrary, Rh/PTAC<sub>1tt600</sub> has some oxygen-free carbon sites, which could provide for an enhancement of activity.

Although it is assumed that alcohol oxidations on metal surfaces proceed via a dehydrogenation mechanism, the precise reaction pathway is still not clear, which further complicates the interpretation of these results. Nevertheless, these experiments clearly demonstrate that the support surface chemistry is a key-factor in the catalytic oxidation of glycerol, at least when using rhodium catalysts.

#### 4 Conclusions

Under the same reactions conditions and for the same support (activated carbon) and preparation method (incipient wetness), the catalytic performance in the selective oxidation of glycerol decreases in the order: Pd > Rh ≫ Pt; on the other hand, Ir and Au are not active. Contrarily to the other catalysts prepared by the conventional method, the gold catalyst presented low particle dispersion. This can explain its inactivity once well-dispersed gold nanoparticles are required in order to obtain an active catalyst. This can be achieved by using a sol immobilisation method of preparation. Palladium and rhodium showed high activities, whereas platinum was rapidly deactivated due to oxygen poisoning. The rhodium catalyst, as far as we know reported for the first time in the present work as active for the reaction, was found to be very promising, namely taking into account its simple preparation method. Additionally, the influence of the surface chemical properties of the support on the activity of this catalyst was clearly demonstrated, being concluded that the presence of acid groups are prejudicial. Particularly, carboxylic acids and anhydrides appeared to be the most detrimental groups. The prepared catalysts lead to a

high total selectivity to products of commercial interest (about 80%).

**Acknowledgments** This work was carried out with support of Fundação para a Ciência e a Tecnologia (FCT) under research fellowship BD/45280/2008 (for EGR), CIENCIA 2007 program (for SACC) and by FCT/FEDER in the framework of Program COM-PETE (project PTDC/EQU-ERQ/101456/2008).

#### References

1. Ma F, Hanna MA (1999) *Bioresour Technol* 70:1
2. Zhou CHC, Beltramini JN, Fan YX, Lu GQM (2008) *Chem Soc Rev* 37:527
3. Haas MJ, McAloon AJ, Yee WC, Foglia TA (2006) *Bioresour Technol* 97:671
4. Behr A, Eilting J, Irawadi K, Leschinski J, Lindner F (2008) *Green Chem* 10:13
5. Pagliaro M, Ciriminna R, Kimura H, Rossi M, Della Pina C (2007) *Angew Chem Int Ed* 46:4434
6. Golz-Berner K, Zastrow L (2007) United States Patent Application # 10/570,031
7. Brandner A, Lehnert K, Bienholz A, Lucas M, Claus P (2009) *Top Catal* 52:278
8. McMorn P, Roberts G, Hutchings GJ (1999) *Catal Lett* 63:193
9. Carrettin S, McMorn P, Johnston P, Griffin K, Kiely CJ, Hutchings GJ (2003) *Phys Chem Chem Phys* 5:1329
10. Demirel-Gülen S, Lucas M, Claus P (2005) *Catal Today* 102–103:166
11. Garcia R, Besson M, Gallezot P (1995) *Appl Catal A* 127:165
12. Porta F, Prati L (2004) *J Catal* 224:397
13. Gao J, Liang D, Chen P, Hou ZY, Zheng XM (2009) *Catal Lett* 130:185
14. Bianchi CL, Canton P, Dimitratos N, Porta F, Prati L (2005) *Catal Today* 102:203
15. Musialska K, Finocchio E, Sobczak I, Busca G, Wojcieszak R, Gaigneaux E, Ziolek M (2010) *Appl Catal A* 384:70
16. Besson M, Gallezot P (2000) *Catal Today* 57:127
17. Prati L, Rossi M (1998) *J Catal* 176:552
18. Bond GC, Thompson DT (1999) *Catal Rev Sci Eng* 41:319
19. Onal Y, Schimpf S, Claus P (2004) *J Catal* 223:122
20. Figueiredo JL, Pereira MFR, Freitas MMA, Órfão JJM (1999) *Carbon* 37:1379
21. Figueiredo JL, Pereira MFR, Freitas MMA, Órfão JJM (2007) *Ind Eng Chem Res* 46:4110
22. Papirer E, Li S, Donnet JB (1987) *Carbon* 25:243
23. Rivera-Utrilla J, Bautista-Toledo I, Ferro-García MA, Moreno-Castilla C (2001) *J Chem Technol Biotechnol* 76:1209
24. Gómez-Serrano V, Acedo-Ramos M, López-Peinado AJ, Valenzuela-Calahorra C (1997) *Thermochim Acta* 291:109
25. Tangsathitkulchai C, Ngernyen Y, Tangsathitkulchai M (2009) *Korean J Chem Eng* 26:1341
26. Moreno-Castilla C, Lopez-Ramon MV, Carrasco-Marin F (2000) *Carbon* 38:1995
27. Menendez JA, Phillips J, Xia B, Radovic LR (1996) *Langmuir* 12:4404
28. Leon y Leon CA, Solar JM, Calemma V, Radovic LR (1992) *Carbon* 30:797
29. Soares OSGP, Órfão JJM, Pereira MFR (2009) *Appl Catal B* 91:441
30. Carabineiro SAC, Thompson DT, (2007) In: Heiz U, Landman U (ed) *Nanocatalysis*, Springer-Verlag, Berlin Heidelberg, ch.6
31. Ryndin YA, Alekseev OS, Simonov PA, Likholobov VA (1989) *J Mol Catal* 55:109

32. Beck A, Horvath A, Stefler G, Scurrall MS, Guzzi L (2009) *Top Catal* 52:912
33. van Dam HE, Wisse LJ, Van Bakkum H (1990) *Appl Catal* 61:187
34. Vinke P, van Dam HE, Van Bakkum H (1990) In: Centi G, Trifiro F (ed) *New developments in selective oxidation*, vol 55. Elsevier, Amsterdam
35. Besson M, Gallezot P (2003) *Catal Today* 81:547
36. Vleeming JH, Kuster BFM, Marin GB (1997) *Catal Lett* 46:187
37. Peereboom L, Koenigsknecht B, Hunter M, Jackson JE, Miller DJ (2007) *Carbon* 45:579